Published in final edited form as:
Exp Eye Res. 2010 December ; 91(6): 866–875. doi:10.1016/j.exer.2010.09.009.

The *In Vitro* Inflation Response of Mouse Sclera

Kristin M. Myers[1], **Frances E. Cone**[2], **Harry A. Quigley**[2], **Scott Gelman**[2], **Mary E. Pease**[2], and **Thao D. Nguyen**[1]

[1] Department of Mechanical Engineering, Johns Hopkins University, Baltimore, MD USA

[2] Glaucoma Research Laboratory, Wilmer Ophthalmological Institute, Johns Hopkins University School of Medicine, Baltimore, MD USA

Abstract

The purpose of this research was to develop a reliable and repeatable inflation protocol to measure the scleral inflation response of mouse eyes to elevations in intraocular pressure (IOP), comparing the inflation response exhibited by the sclera of younger and older C57BL/6 mice. Whole, enucleated eyes from younger (2 month) and older (11 month) C57BL/6 mice were mounted by the cornea on a custom fixture and inflated according to a load-unload, ramp-hold pressurization regimen via a cannula connected to a saline-filled programmable syringe pump. First, the tissue was submitted to three load-unload cycles from 6 mmHg to 15 mmHg at a rate of 0.25 mmHg/s with ten minutes of recovery between cycles. Next the tissue was submitted to a series of ramp-hold tests to measure the creep behavior at different pressure levels. For each ramp-hold test, the tissue was loaded from 6 mmHg to the set pressure at a rate of 0.25 mmHg/s and held for 30 minutes, and then the specimens were unloaded to 6mmHg for 10 minutes. This sequence was repeated for set pressures of: 10.5, 15, 22.5, 30, 37.5, and 45 mmHg. Scleral displacement was measured using digital image correlation (DIC), and fresh scleral thickness was measured optically for each specimen after testing. For comparison, scleral thickness was measured on untested fresh tissue and epoxy-fixed tissue from age-matched animals. Comparing the apex displacement of the different aged specimens, the sclera of older animals had a statistically significant stiffer response to pressurization than the sclera of younger animals. The stiffness of the pressure-displacement response of the apex measured in the small-strain (6-15 mmHg) and the large-strain (37.5-45 mmHg) regime, respectively, were 287 ± 100 mmHg/mm and 2381 ± 191 mmHg/mm for the older tissue and 193 ± 40 mmHg/mm and 1454 ± 93 mmHg/mm for the younger tissue (Student t-test, $p < 0.05$). The scleral thickness varied regionally, being thickest in the peripapillary region and thinnest at the equator. Fresh scleral thickness did not differ significantly by age in this group of animals. This study presents a reliable inflation test protocol to measure the mechanical properties of mouse sclera. The inflation methodology was sensitive enough to measure scleral response to changes in IOP elevations between younger and older C57BL/6 mice. Further, the specimen-specific scleral displacement profile and thickness measurements will enable future development of specimen-specific finite element models to analyze the inflation data for material properties.

Correspondence: Thao D. Nguyen Johns Hopkins University 3400 North Charles St. Latrobe 125 Baltimore, MD 21218 vicky.nguyen@jhu.edu Phone: (410) 516-4538 Fax: (410) 516-7254.

Keywords

sclera; inflation; mechanical properties; mouse; glaucoma; myopia

Introduction

The load-bearing eye wall consists of the collagen-rich sclera and cornea, which act as a protective shell for the inner structures of the eye. Previous mechanical testing and modeling of scleral tissue have suggested that changes to the mechanical behavior of the sclera are related to the development and progression of myopic (McBrien et al. 2001) and glaucomatous damage (Burgoyne et al., 2005; Ethier, 2006; Nickells, 2007). To understand how the mechanical behavior of the sclera play a role in glaucoma, we are using mouse models to study the relationship between the collagen/elastin structure and the mechanical properties of the sclera and their associations with glaucomatous optic neuropathy. Initial anatomic investigations have shown that the structure of the mouse sclera is similar in several respects to that of human sclera (Gelman et al., 2009; Watson and Young, 2004; Quigley et al., 1991a, 1991b). In addition, mouse models provide important opportunities to manipulate the composition and structure of the ocular connective tissues by chemically treating the animals *in vivo* or by gene knockout techniques. In this paper, we present a robust and repeatable *in vitro* inflation method to measure and compare the inflation response of the mouse sclera to elevations in IOP. In addition, we present a new method for measuring fresh-tissue scleral thickness of the mouse eye.

Previous mechanical testing on intact human (Woo et al., 1972), porcine (Girard et al., 2008), monkey (Girard et al., 2009) and rabbit scleral tissue (Greene and McMahon, 1979) established that the sclera deforms nonlinearly in response to pressure elevation and creeps over long periods of time in response to a constant elevated pressure. Age-related mechanical and biochemical studies showed that scleral tissue stiffens with age (Avetisov et al. 1984; Frigberg and Lace, 1988; Girard et al., 2009) and that there is an increase in the intermolecular collagen crosslinks in mature sclera compared to younger sclera (Curtin, 1969; Avetisov et al. 1984; Keeley et al., 1984; Ihanamaki et al., 2001; Watson and Young, 2004). Indirect measurements suggest that human glaucoma eyes are stiffer than age-matched controls (Hommer et al. 2008), and experimental glaucoma in monkeys leads to an increase in the equilibrium modulus of the sclera (Downs et al. 2005). To extend such observations to age and disease-related scleral changes in mice, improvements to the mechanical testing methods are needed to include protocols that can measure the time-dependent inflation behavior of an intact eye. In addition, studies that are applicable to smaller eyes would permit the expansion of such research to transgenic mouse models.

This paper presents the first experimental protocol for *in vitro* inflation testing of intact mouse sclera and reports the inflation response and fresh-tissue thickness measurements comparing younger (2 month) and older (11 month) C57BL/6 mouse eye specimens. The inflation protocol preserves the curvature of the sclera, measures and controls IOP accurately, captures non-equilibrium inflation displacements, and accounts for scleral geometry.

Materials and Methods

Animals

We measured the dimensions of the eye in 19 C56BL/6 mice, 10 of which were 2 month old and 9 at 11 months of age. Of these 19 mice, 13 underwent inflation testing: seven 2 month old mice and six 11 month old mice, while the other 6 were not used due to improper gluing

to the fixture or incomplete flow through the cannula (see below). In the inflation studies for each mouse, one eye was inflation-tested and then measured for fresh-tissue scleral thickness while the fellow eye was used for fresh-tissue scleral thickness measurements only. Of the 13 inflation specimens, 11 completed the full scleral displacement tracking (five 2 month mice and six 11 month mice), while the other two specimens were excluded because of artifacts in the DIC imaging. Artifacts include small dust particles or debris that obstruct the scleral edge in the video image.

An additional five C57BL/6 animals at an average age of 5 months were used for the measurements of sclera thickness in epoxy-embedded sections. All animals were treated with protocols approved and monitored by the Animal Care Committee of the Johns Hopkins University School of Medicine. Animals were housed with a 14 h light/10 h dark cycle with standard food and water *ad libitum*.

Inflation Test

Animals were anesthetized with a mixture of ketamine (Fort Dodge Animal Health, Fort Dodge, IA), xylazine (VedCo Inc., Saint Joseph, MO), and acepromazine (Phoenix Pharmaceuticals, Burlingame, CA) at 50, 10 and 2 mg/kg, respectively. The superior pole of the cornea was marked and the eyes were enucleated. The animals were then euthanized by cervical dislocation. Enucleated eyes were cleaned of extraocular tissues and the axial length and width were measured with a digital caliper (Instant Read Out Digital Caliper, Electron Microscopy Sciences, Hatfield, PA, USA). The axial length was measured from the center of the cornea to a position just temporal to the optic nerve, while width was measured at the largest dimension at the equator, midway between cornea and optic nerve, in both the nasal-temporal axis and the superior-inferior axis. The cornea was then glued into a custom fixture using slow-drying cyanoacrylate glue. Care was taken to avoid spread of glue to the sclera and the unglued surface was kept moist with phosphate buffered saline (PBS) as the glue dried. Then, the anterior chamber was cannulated just anterior to the limbus with a custom 30 gauge needle assembly. The needle was glued to the fixture, and the entire fixture assembly with the eye was placed in a PBS bath underneath a dissecting microscope (Zeiss Greybody, Carl Zeiss Microimaging, Thornwood, NY). The specimen was oriented with the superior pole toward the camera, providing a view of the nasal-temporal sclera in the measuring plane (Fig. 1). Specimens were discarded if the glue extended posterior to the limbus, if the limbus did not align with the holder edge, or if the cannula did not have clearly open flow in and out of the eye - such as might be caused by cannulating into the lens. To test if the cannula did not have an open flow, the pressure was raised slightly just after cannulation, and the sclera was inspected to see if the surface wrinkles unfolded.

IOP was slowly increased by syringe actuation to a reference pressure of 6 mmHg, which we found to be the lowest pressure at which the sclera was no longer visibly wrinkled, and the eye was allowed to equilibrate for 15 minutes. Then, eyes were inflated in a series of load-unload and ramp-hold creep tests. First, the eyes were loaded from 6 mmHg to 15 mmHg (at 0.25 mmHg/s) and then immediately unloaded to 6 mmHg for 5 minutes. This load-unload was repeated two more times. Specimens were then loaded to 10.5 mmHg for 30 minutes and unloaded to 6 mmHg for 10 minutes. This creep test was repeated to pressure levels of 15, 22.5, 30, 37.5, and 45 mmHg.

Feedback Pressure Controller

During scleral inflation, IOP was controlled through the cannula and measured with an in-line pressure transducer (Sensotech TJE, 2psi, ±0.002psi). The eye fixture consisted of a disposable polycarbonate (PC) holder fit within a stainless steel chuck. The PC holder had a machined 3 mm diameter, hemispherical cup, custom filed to fit the sample diameter, and a

narrow perpendicular slot to guide needle insertion. Lab tape was used to facilitate needle placement (Figure 1). A pressure feedback controller, programmed in Labview (National Instruments, V8.5), controlled the actuation of a syringe pump (Cavro XL 3000, 5mL) to inject PBS into the cannula line according to the difference between the measured cannula pressure and the desired set pressure. The Labview program employed the built-in proportional controls logic, with the proportional gain set to 1. See Fig. 2 for a diagram of the experimental set-up.

Scleral Displacement

Scleral displacement was measured during inflation using a two-dimensional (2D) digital image correlation (DIC) system, which consisted of a CCD video camera (GRAS-20S4M/C, Pt. Grey Research) attached to the dissecting microscope. The camera imaged at a rate of 0.5Hz with a 5.4μm/pixel resolution. A commercial DIC software package (Vic-2D, Correlated Solutions, Columbia, SC) was used to analyze the images of the inflating specimens for the 2D displacement of the scleral edge. DIC is an optical method that identifies a contrasting grayness pattern in a chosen subset of pixels in comparison to a reference image. The grayness pattern is matched between the deformed images and the reference image to calculate the displacement field (Sutton and McFadden, 2000). Multiple DIC tracking points were placed on the scleral edge of the reference image from points near the ONH to the holder. Figure 3 illustrates a typical sclera specimen with the DIC tracking locations.

The total error for the displacement measurements was calculated by summing the contributions from the uncertainty of the pixel-distance calibration, the resolution of the pressure transducer, and the inherent error of the DIC software. The uncertainty of the extensometer calibration arose from the irresolution of counting the pixels between known markers on a precision ruler. This was determined by taking multiple pixel counts, and the maximum range of the measurement was ± 0.36μm. The displacement error from the pressure transducer resolution was approximated for each specimen by measuring the displacement response to the maximum pressure tolerance of the Sensotech TJE 2psi pressure transducer ±0.002psi (±0.15mmHg). The range of errors was ± 0.44μm for the stiffest specimen to ± 1.5μm for the most compliant specimen. Lastly, the DIC manufacturer reported an overall subpixel resolution of 0.02 times the pixel value resulting in a DIC resolution of ±0.1μm.

Scleral Thickness

For the determination of the fresh-tissue scleral thickness profile, measurements were taken on the inflated specimens and on its fellow control eye. The superior pole was marked on the cornea with spot of cautery without altering the sclera (Acuderm Inc., Ft. Lauderdale, FL). Upon enucleation, eyes were submerged in 0.1M phosphate buffer. Fat and muscle tissue were removed from the exterior of the eye and a 0.5 to 1mm length of optic nerve was left attached to the globe. Using a digital caliper (Electron Microscopy Sciences. Hatfield, PA, ± 0.01mm) and the Zeiss dissecting microscope, globes were measured in both axial length, from anterior to posterior, and width, superior to inferior and nasal to temporal. The superior portion of the sclera was lightly marked using a marker (Kendall-LTP/ Tyco. Mansfield, Massachusetts). With a thin Persona razor blade (American Safety Razor Company, Verona, VA), a small incision was made anterior to the limbus. The cornea, lens and retina/choroid were removed from the eye cup. Tissue was immersed in PBS throughout the measurements. Four slices were made to flatten out the cup. The superior quadrant was removed from the cup by cutting at the peripapillary region anterior to the nerve. The quadrant was then sliced lengthwise, from the peripapillary region to the limbus, into three long and thin strips. Starting with the superior strip adjacent to the nasal side, cross sections were taken at 6

different points, moving from the peripapillary region to the limbus in 0.5mm increments. Three ocular unit measurements were taken per cross section on each of the three strips on a Zeiss Stemi 2000 with the ocular units read through a Zeiss 10x eyepiece (Carl Zeiss Microimaging, Thornwood, NY). Ocular units were then converted into micrometers and the mean was calculated for each cross section and for each region of the eye.

For comparison with the fresh tissue measurements of scleral thickness, sclera from the peripapillary region was epoxy-embedded and its thickness measured in tissue sections. The animals were perfused using 2% paraformaldehyde / 2% glutaraldehyde (Electron Microscopy Sciences, Hatfield, PA) in 0.1M phosphate buffer (Electron Microscopy Sciences, Hatfield, PA). The superior pole was marked with cautery of the cornea, avoiding scleral damage posterior to the limbus. Fat and muscle tissue were removed from the exterior eye, while also preserving the nerve for future analysis of glaucomatous damage. The globe was cut into 4 individual strips: superior, nasal, temporal and inferior. Tissue was placed in 1% osmium (Electron Microscopy Sciences, Hatfield, PA), dehydrated in ascending concentrations of ethanol, and placed in 100% ethanol with 1% uranyl acetate (Electron Microscopy Sciences, Hatfield, PA) for 1 hour. Tissues were embedded using epoxy resin mixture and placed in a 60°C oven for 48 hours. One micron thick sections were taken from each sclera strip, and the tissue was stained using 1% toluidine blue (Electron Microscopy Sciences, Hatfield, PA) and 1% sodium borate (Fisher Scientific, Pittsburgh, PA). Three images were taken using a 100x oil lens from a Zeiss Microscope using a Cool Snap camera (Carl Zeiss Microimaging, Thornwood, NY). Measurements of scleral thickness were taken at three different locations in the peripapillary region using the Metamorph Image Analysis software (Molecular Devices, Downington, PA). A total of nine measurements were used at each of the four quadrants, resulting in a total of 36 measurements per eye.

Results

Scleral Geometry

In globe measurements along the anterior-posterior, nasal-temporal, and inferior-superior diameters, older mouse eyes were significantly larger than younger mouse eyes (Student t-test, $p<0.01$; Table 1). For both the younger and older animals, the anterior-posterior dimension was significantly larger than the other two dimensions (Student t-test, $p<0.01$).

The fresh-tissue scleral thickness measurements from the inflation tested specimens and untested, fellow eyes were collected from 6 regions, numbered from 1 (peripapillary) through 6 (limbus), every 0.5mm. The sclera was thickest in the peripapillary region (Student t-test, $p < 0.05$; Table 2). The limbal region (#6) was statistically thicker than scleral locations 3, 4, and 5. The limbal region was thinner than the peripapillary region, but the difference was not statistically different (Student t-test, $p < 0.05$). There was no statistically significant difference in the scleral thickness profile between younger and older C57BL/6 animals, nor between the mechanically-tested and untested eye sclera (Student t-test, all p values > 0.05).

Epoxy-embedded tissue section measurements of scleral thickness were 51% thinner than fresh tissue measurement. For example, peripapillary scleral thickness in sections was a mean of 31.2 ± 3.0 μm, a significant difference from the fresh-tissue measurements reported for region #1 in Table 2 (Student t-test, $p<0.01$). Since this difference was likely due to shrinkage from fixation, embedding and sectioning, we advocate the use of fresh thickness measurements in subsequent analysis.

Response to Inflation

Apex displacement response—Apex displacement, defined as the average displacement for two DIC tracking points in the peripapillary region, one each on either side of the optic nerve stump, was used as the initial measure of the inflation response (Figure 3). In the first loading ramp, from P_o to 15mmHg, the average apex displacement response in younger eyes was more compliant than for older eyes. The stiffness of the pressure-displacement response, measured as the change in pressure divided by apex displacement, for this initial loading test was 228 ± 59 mmHg/mm and 323 ± 79 mmHg/mm for the younger and older eyes, respectively. The *stiffness* measurements reported here represent the combined contributions of the scleral geometry and scleral material properties, and the stiffness difference between the younger and older tissue were statistically significant, taking into account the error of the pressure transducer and the standard deviation of displacement measurements (Student t-test, $p<0.05$; Figure 4A). The final loading ramp (P_o to 45mmHg) showed a nonlinear relationship between apex displacement and pressure, with an initial compliant response and a stiffening of the tissue with pressure increase (Figure 4B; Table 3). The nonlinearity was present in both younger and older eyes, evident by the statistically significant increase in the slope of the pressure-displacement response with increases in pressure (except between 30 and 45 mmHg) for each age group (Student t-test, all p values < 0.05; Table 3). Further, the younger sclera was again significantly more compliant than older sclera, when comparing the stiffness of the apex pressure-displacement response between the two ages at different pressure regimes (Student t-test, all p values < 0.05; Table 3). Lastly, there was a significant difference in stiffness of the apex pressure-displacement response for both age groups measured in the P_o to 15mmHg regime when comparing the initial loading test (Fig. 4A) and the last loading (Fig. 4B), indicating a slight softening during the ramp-hold tests (Student t-test, $p<0.05$).). However, the measured softening effect between the first and last loading was small compared to the amount of stiffening measured for each age group.

In the 15, 30, and 45 mmHg ramp-hold (creep) tests, we again used the averaged displacements of two peripapillary locations as the outcome. There was evidence of time-dependent creep for both younger and older sclera for all pressure levels, with the creep rates being significantly larger than zero (Table 4; Student t-test, $p < 0.05$). There was no statistically significant difference for the creep rates between the younger and older tissue and between the different hold pressures (Student t-test, $p > 0.05$).

Displacement of scleral profile—To measure the behavior of the entire scleral outline under inflation, we tracked the *x* - and *y* - displacement of up to 20 locations on either perimeter of the sclera, at specific DIC pixel points chosen approximately 100μm apart in the *y*-direction (Figure 3). In presenting the scleral displacement profile at 7 different pressures (10.5, 15, 22.5, 30, 37.5, and 45mmHg), we show the scleral edge tracking for one-half of the specimen using the convention that the y-axis is displacement posteriorly (away from the cornea) and x-axis displacement is the circumferential expansion. The other half of the scleral displacement profile, not shown, had a similar behavior and was omitted for clarity. Scleral displacement plots for additional specimens plotted in this way are found in the Appendix. In general, for both young and old tissue, axial (y-axis) displacement was larger than circumferential (x-axis) displacement. The location of maximum axial displacement varied among specimens. The largest gradient in y-axis displacements (indicating strain) occurred closer to the holder. The significance of these findings will be explored by comparing material parameters that will be generated with finite element modeling in our future work.

Discussion

We have developed a mechanical testing method to measure the inflation response of the sclera in the intact, enucleated mouse eye. Further, we measured the thickness of fresh sclera at multiple locations from the posterior pole to the limbus. These methods generated scleral inflation displacement profiles of younger and older C57BL/6 mice, permitting future studies that will estimate the differences in scleral inflation response due to age, mouse type, and induced and spontaneous glaucoma. This approach will support our current modeling efforts to quantify the nonlinear, time-dependent and heterogeneous scleral material properties.

Our main motivation for the development of these scleral mechanical testing methods was to understand the development of glaucoma. Glaucoma is a leading cause of blindness in the world, and it is projected that 80 million people will suffer from open angle and angle closure glaucoma by 2020 (Quigley and Broman, 2006). The disease manifests as the progressive loss of retinal ganglion cells (RGCs), with damage to their axons in the optic nerve head (ONH) (Quigley et al., 1981). The injury from glaucoma is related to the level of intraocular pressure (IOP), which generates tensile stresses in the sclera that are transmitted to the ONH, potentially subjecting the RGC axons, glial cells, and supportive capillaries to damaging deformation. It is increasingly recognized that the biomechanical response of the sclera is important to the development and progression of RGC damage (Burgoyne et al., 2005; Ethier, 2006; Nickells, 2007). Finite element models of the posterior globe showed that the elastic modulus of the peripapillary sclera has a larger influence on the ONH deformation response to acute IOP elevation than the mechanical properties of the ONH tissues, or the dimensions and relative position of the ONH and sclera (Sigal et al., 2004, 2005, 2009). Clinical and laboratory experiments have also revealed differences in the material properties of normal and diseased sclera. Hommer et al. (2008) measured the *in vivo* ocular expansion induced by blood pressure pulsation and reported that the eyes of glaucoma patients exhibited a higher estimated ocular stiffness than those of non-glaucoma patients. Similarly, Downs et al. (2005) showed that the stress relaxation behavior measured by uniaxial tensile tests of monkey sclera with laboratory-induced glaucoma displayed a larger modulus compared to the sclera of normal monkey eyes. The Hommer et al. and Downs et al. studies suggested that the mechanical behavior of the sclera differ with glaucoma. However, the uniaxial loading of strip specimens and the associated boundary conditions may not represent the complex loading conditions experienced by the intact sclera. Further, the cutting of the sclera into strips may alter collagen fibril structure and clearly disrupts the natural curvature of the tissue. In the Hommer study, the ocular expansion measurement is a systems measurement that combined the effects of ocular geometry and the material properties of the sclera, cornea, and internal ocular tissues. Further, the ocular volume measurements were based on the assumption that the ocular rigidity was equal for all subjects. Our methodology has the advantage of preserving the curvature of the intact tissue. Further, the DIC method allows for the capture of the instantaneous loading response and time-dependent creep of the inflating eye, which accommodates our current viscoelastic modeling effort. Our future plans include conducting inflations studies on a spontaneous glaucoma mouse model DBA/2J and induced glaucoma mouse models.

We found that the thickness of fresh scleral sections was largest in the peripapillary region, thinnest in the equator, and intermediate at the limbus. This scleral thickness profile for the mouse is similar to that in the human sclera (Olsen et al., 1988; Watson and Young, 2004; Norman et al., 2010), though the absolute thickness is an order of magnitude thinner in the mouse. Scleral measurements in epoxy-embedded tissue sections were dramatically thinner, reflecting the shrinkage due to fixation, dehydration, and embedding. Available optical or

ultrasonic measuring instruments (pachymeters) could not accurately measure fresh mouse sclera due to its extreme thinness. Thus, for future use in finite element modeling, we will use the fresh measurement system presented here to estimate the *in vivo* hydrated thickness of the scleral. Intererestingly, the thickness of eyes that had undergone inflation testing was not significantly different from fellow eyes that were not inflated, suggesting that permanent alterations do not occur within the time frame of several hours of testing.

The mechanical response of the sclera to increases in pressure, given by the pressure-displacement curves for both younger and older specimens, was non-linear and time-dependent. The nonlinearity of the inflation response was characterized by a typical J-shaped pressure-displacement relationship, noted for other classes of collagenous soft tissues, with an initial compliant response followed by a dramatic stiffening with increases in pressure. The time-dependent response was characterized by creep of the posterior sclera during a constant pressure. The mechanical behavior of soft connective tissues is determined by the composition, structure, and mechanical properties of its extracellular matrix (ECM) components. The connective tissue of the sclera is composed of type I and III collagen fibrils, organized into lamellae, and elastin fibers that are crosslinked and embedded in a hydrated proteoglycan matrix (Curtin 1969; Watson and Young, 2004; Quigley et al., 1991a, 1991b; Young, 1985). The microstructure of the scleral connective tissue is heterogeneous, with regional changes in the composition and arrangement of the ECM components (Quigley et al., 1991a, 1991b). For example, recent work in our lab shows that elastin is confined to the posterior sclera of the mouse, with a dense ring in the peripapillary sclera around the optic nerve head (Gelman et al., 2009). The mechanical response of the sclera to changes in IOP depends on the complex interaction of the heterogeneous ECM components. In other classes of soft connective tissues, such as the tendon, the small-strain toe region coincides with the straightening of wavy collagen fibers and is dominated by the stress response of the elastin fibers and proteoglycan matrix (Ventre et al., 2009; Fung, 1993). The non-linear stiffening at larger strains is thought to be related to the gradual recruitment and elongation of the stiffer collagen fibers (Fung 1993).

Age-related differences in the ECM structure and the mechanical properties of collagenous tissues have been well studied. Specifically, previous biochemical analysis on human and mouse scleral tissue established that there is a decrease in the collagen turnover rate accompanied by an increase in the intermolecular collagen crosslink density and fiber diameter for mature collagen fibrils when compared to younger fibrils, resulting in an increased resistance to enzymatic digestion (Curtin, 1969; Keeley et al., 1984; Ihanamaki et al., 2001; Watson and Young, 2004). This increase in both the enzymatic and nonenzymatic intermolecular collagen crosslink density would increase its tensile loading strength (Lodish, 2004). It can be hypothesized that this increase in collagen crosslinking and the reduction of collagen turnover provides for a stiffening mechanism for the mature scleral tissue. Mechanical studies on the cornea (Elsheikh et al., 2007) and sclera (Frigberg and Lace, 1988; Girard et al., 2009) confirmed this stiffening by comparing the mechanical response of young and old scleral tissue from porcine and humans. Conducting tensile strip tests of human scleral specimens, Friberg et al. (1988) observed that the scleral modulus of elasticity increased with age. Mostly recently, Girard et al. (2009) conducted inflation tests on intact scleral tissue from old and young rhesus monkeys and also showed that the tissue stiffens with age. In the study presented here, we found a statistically significant difference in the inflation response between younger and older C57BL/6 mouse sclera, with younger tissue more compliant than older specimens from the same mouse strain. In addition, the creep rate of the younger tissue had a significant dependence on the pressure level, where the older tissue did not. The inflation response reported by the pressure-displacement curves in this study give further evidence that age has a stiffening effect on the inflation response of the mouse sclera.

Tracking the scleral edge of multiple young and old scleral specimens revealed that the location of maximum axial elongation varied between specimens and was not necessarily located at the peripapillary sclera next to the ONH (apex). In addition, the displacement in the *x*-direction (circumferential expansion) was less than the *y*-direction (axial elongation), and the circumferential expansion was nearly zero in the peripapillary region. We plan to construct a finite element model of mouse scleral geometry, its boundary conditions and loading conditions. This model will help to understand the specimen-specific shape of the scleral displacement profile and the anisotropy between the *x*- and *y*-displacement response. The anisotropy of the displacement response could be influenced by a combination of the boundary conditions at the limbus imposed by the fixture and the intrinsic anisotropy of the scleral ECM microstructure. The axial scleral displacement profile could be influenced by a number of different factors, including: the shape of the scleral shell, the size and material properties of the ONH, the scleral thickness profile, tissue anisotropy resulting from the preferred orientation of ECM fiber bundles, and the heterogeneity of scleral material properties.

The experimental results and methodology presented here had limitations, and improvements to the protocol are currently being implemented to address these concerns. The methods detailed in this paper provide an initial framework for studying the inflation response of an intact mouse eye, moving toward a full analysis of the stress and strain of the posterior sclera. We are currently building a finite element model to include the specimen-specific thickness variation and regional differences in the connective tissue microstructure. This will involve fitting a non-linear viscoelastic model to the pressure-displacement relationships presented in this paper to generate material parameters. Our present data provide 2-dimensional displacement results and assume axisymmetry. This assumption must be validated either by conducting a three-dimensional inflation test or by inflating the specimen rotated along the optical axis. We have utilized 3-dimensional displacement methods in bovine cornea (Boyce et al., 2008; Nguyen et al., 2008) and sclera (Myers et al., 2010) and human sclera (B. Coudriller, personal communication, 2010), and we are testing methods applicable to the mouse eye. In addition, the creep rates measured *in vitro* may not ideally reflect the *in vivo* behavior of the sclera. We have found that induced, chronic IOP elevation causes permanent axial and circumferential elongation of the mouse eye (F. Cone, personal communication, 2010). However, in the living eye, short-term responses would be accompanied by active tissue remodeling and other local processes that are likely to be inoperative *in vitro*. Nonetheless, *in vitro* creep rates can be productively compared between strains of mice, between younger and older animals, and after experimental alterations to achieve a first approximation of the determinants of the baseline viscoelastic nature of the sclera.

We have developed a protocol for the inflation test of mouse sclera and presented the detailed mechanical behavior of the sclera in younger and older C57BL/6 mice. This mechanical test method paired with histological measurements provides a framework for studying the relationship between the structure and mechanical properties of the connective tissues of the eye and their associations with age and disease.

Appendix

Scleral displacement profiles from the additional 2 month C57BL/6 mouse eyes:

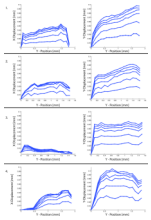

Scleral displacement profiles from the additional 11 month C57BL/6 mouse eyes:

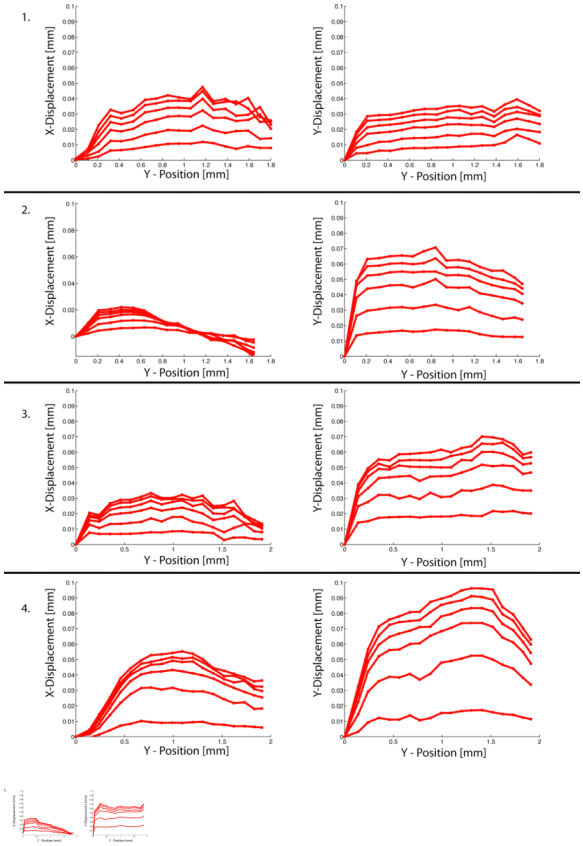

References

Avetisov ES, et al. A study of biochemical and biomechanical qualities of normal and myopic eye sclera in humans of different age groups. Metab. Pediatr. Syst. Ophthalmol 1984;7:183–188. [PubMed: 6678372]

Boyce BL, et al. Full-field deformation of bovine cornea under constrained inflation conditions. Biomat 2008;29(28):3896–3904.

Burgoyne CF, et al. The optic nerve head as a biomechanical structure: a new paradigm for understanding the role of IOP-related stress and strain in the pathophysiology of glaucomatous optic nerve head damage. Prog. Retin. Eye. Res 2005;24:39–73. [PubMed: 15555526]

Curtin B. Physiopathologic aspects of scleral stress-strain. Tr. Am. Ophth. Soc 1969;67:417–461. [PubMed: 5381306]

Downs JC, et al. Viscoelastic material properties of the peripapillary sclera in normal and early-glaucoma monkey eyes. Invest. Ophthalmol. Vis. Sci 2005;46:540–546. [PubMed: 15671280]

Elsheikh A, et al. Assessment of corneal biomechanical properties and their variation with age. Curr. Eye Res 2007;32:11–19. [PubMed: 17364730]

Ethier CR. Scleral biomechanics and glaucoma-a connection? Can. J. Ophthalmol 2006;41:9–11. [PubMed: 16462866]

Friberg TR, Lace JW. A comparison of the elastic properties of human choroid and sclera. Exp. Eye Res 1988;47:429–436. [PubMed: 3181326]

Fung, YC. Biomechanics: mechanical properties of living tissues. Springer-Verlag; New York: 1993.

Gelman S, et al. The presence and distribution of elastin in the mouse eye. Exp. Eye Res 2010;90:210–215. [PubMed: 19853602]

Girard MJA, et al. Experimental surface strain mapping of porcine peripapillary sclera due to elevations of intraocular pressure. J. Biomech. Eng 2008;130(4):041017. [PubMed: 18601459]

Girard MJA, et al. Scleral biomechanics in aging monkey eye. Invest. Ophthalmol. Vis. Sci 2009;50:5226–5237. [PubMed: 19494203]

Greene PR, McMahon TA. Scleral creep vs temperature and pressure in vitro. Exp. Eye Res 1979;29:527–537. [PubMed: 527689]

Hernandez MR, Luo XX, Andrzejewska W, Neufeld AH. Age-related changes in the extracellular matrix of the human optic nerve head. Am. J. Ophthalmol 1989;107:476–484. [PubMed: 2653045]

Hernandez MR. Ultrastructural immunocytochemical analysis of elastin in the human lamina cribrosa. Changes in elastic fibers in primary open-angle glaucoma. Invest. Ophthalmol. Vis. Sci 1992;33:2891–2903. [PubMed: 1526740]

Hommer A, Fuchsjager-Mayrl G, Resch H, Vass C, Garhofer G, Schmetterer L. Estimation of ocular rigidity based on measurements of pulse amplitude using pneumotonometry and fundus pulse using laser interferometry in glaucoma. Invest. Ophthalmol. Vis. Sci 2008;49:4046–4050. [PubMed: 18487379]

Ihanamaki T, et al. Age-dependent changes in the expression of matrix components in the mouse. Exp. Eye Res 2001;72:423–431. [PubMed: 11273670]

John SW, et al. Intraocular pressure in inbred mouse strains. Invest. Ophthalmol. Vis. Sci 1997;38:249–253. [PubMed: 9008647]

John SW. Mechanistic insights into glaucoma provided by experimental genetics. The Cogan Lecture. Invest. Ophthalmol. Vis. Sci 2005;46:2650–2661.

Keeley FW, Morin JD, Vesely S. Characterization of collagen from normal human sclera. Exp. Eye Res 1984;39:533–542. [PubMed: 6519194]

McBrien NA, Lawlor P, Gentle A. Structural and ultrastructural changes to the sclera in a mammalian model of high myopia. Invest. Ophthalmol. Vis. Sci 2001;42:2179–2187. [PubMed: 11527928]

Myers KM, et al. The inflation response of bovine sclera. Acta Biomater. submission in review.

Lodish, et al. Molecular Cell Biology. fifth ed.. W.H. Freeman and Company; New York: 2004. p. 218

Nickells RW. From ocular hypertension to ganglion cell death: a theoretical sequence of events leading to glaucoma. Can. J. Ophthalmol 2007;42:278–287. [PubMed: 17392853]

Nguyen TD, Jones RE, Boyce BL. A nonlinear anisotropic viscoelastic model for the tensile behavior of the corneal stroma. J Biomech. Eng 2008;130:041020. [PubMed: 18601462]

Norman RE, et al. Dimensions of the human sclera: Thickness measurement and regional changes with axial length. Exp. Eye Res 2010;90(2):277–284. [PubMed: 19900442]

Olsen TW, et al. Human sclera: thickness and surface area. Am. J. Ophthalmol 1998;124:237–241. [PubMed: 9467451]

Quigley HA, et al. Optic nerve damage in human glaucoma. II. The site of injury and susceptibility to damage. Arch. Ophthalmol 1981;99:635–49. [PubMed: 6164357]

Quigley HA, Brown A, Dorman-Pease ME. Alterations in elastin of the optic nerve head in human and experimental glaucoma. Br. J. Ophthalmol 1991a;75:552–7. [PubMed: 1911659]

Quigley HA, Dorman-Pease ME, Brown AE. Quantitative study of collagen and elastin of the optic nerve head and sclera in human and experimental monkey glaucoma. Curr. Eye Res 1991b; 10:877–88. [PubMed: 1790718]

Quigley HA, Pease ME, Thibault D. Change in the appearance of elastin in the lamina cribrosa of glaucomatous optic nerve heads. Graefe's Arch Clin Exp Ophthalmol 1994;232:257–61. [PubMed: 8045433]

Quigley EN, et al. Quantitative studies of elastin in the optic nerve heads of persons with open-angle glaucoma. Ophthalmology 1996;103:1680–5. [PubMed: 8874442]

Quigley HA, Broman AT. The number of people with glaucoma worldwide in 2010 and 2020. Br. J. Ophthalmol 2006;90:262–267. [PubMed: 16488940]

Pena JD, et al. Elastosis of the lamina cribrosa in glaucomatous optic neuropathy. Exp. Eye Res 1998;67:517–524. [PubMed: 9878213]

Sigal IA, et al. Finite element modeling of optic nerve head biomechanics. Invest Ophthalmol 2004;45:4378–4387.

Sigal IA, Flanagan JG, Ethier CR. Factors influencing optic nerve head biomechanics. Invest. Ophthalmol. Vis. Sci 2005;46:4189–4199. [PubMed: 16249498]

Sigal IA, Flanagan JG, Ethier CR. Modeling individual-specific human optic nerve head biomechanics. Part I: IOP-induced deformations and influence of geometry. Biomechan. Model Mechanobiol 2009;8:85–98.

Sutton MA, McFadden C. Development of a methodology for non-contacting strain measurements in fluid environments using computer vision. Opt. Lasers Eng 2000;22:367–377.

Ventre M, Mollica F, Netti PA. The effect of composition and microstructure on the viscoelastic properties of dermis. J. Biomech 2009;42:430–435. [PubMed: 19159885]

Watson PG, Young RD. Scleral structure, organization and disease. A review. Exp. Eye Res 2004;78:609–623. [PubMed: 15106941]

Woo SL-Y, et al. Nonlinear material properties of intact cornea and sclera. Exp. Eye Res 1972;14:29–39. [PubMed: 5039845]

Young RD. The ultrastructure organization of proteoglycans and collagen in human and rabbit scleral matrix. J. Cell Sci 1985;74:95–104. [PubMed: 4030913]

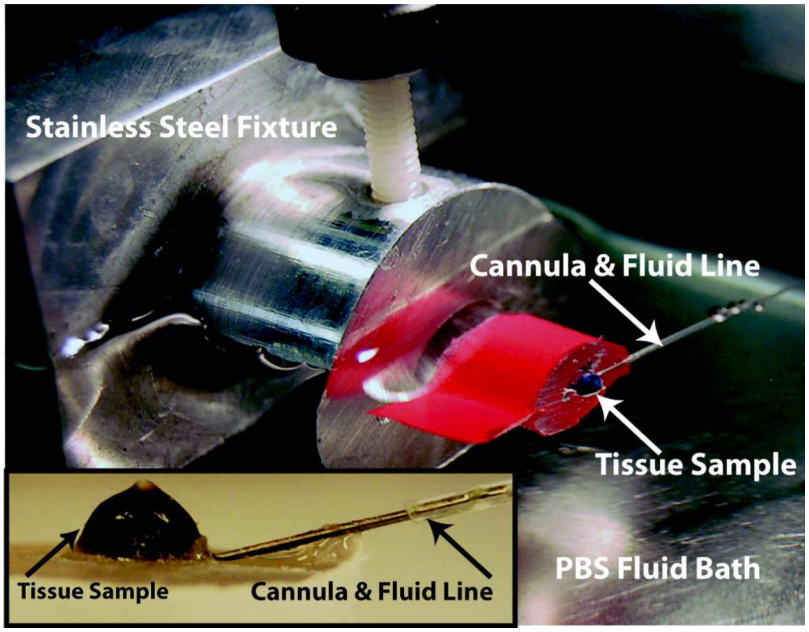

Figure 1.
Specimen in the inflation testing fixture. The inset depicts a close-up of the tissue sample in the holder, with the cannula angled slightly to avoid the lens and to properly insert into the anterior chamber.

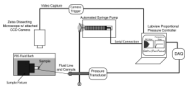

Figure 2.

Experimental set-up. The eye is tested in a PBS bath and its IOP is measured and controlled via an active pressure-feedback controller through the attached cannula. The pressure of the sample is recorded on a computer (Dell Precision T7500) through a National Instruments data acquisition system (NI 9237 DAQ). The automated syringe pump (Cavro XL 3000, 5mL) is programmed, through a Labview proportional controller (National Instruments, V8.5), to dispense or aspirate PBS into the cannula depending on the difference between the measured pressure (P_{actual}) and the set pressure (P_{set}). The CCD video camera (GRAS-20S4M/C, Pt. Grey Research) attached to the dissecting microscope (Zeiss Greybody) records images during inflation testing, and the digital image correlation software (Vic 2D, Correlated Solutions) measures scleral displacement.

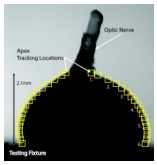

Figure 3.

A digital image correlation (DIC) video snapshot of a 2 month old C57BL/6 mouse sclera in the testing fixture underneath the dissecting microscope in the reference configuration. The boxes represent the digital image correlation (DIC) tracking subset locations for 2D tracking of the point relative to its position in the reference configuration, and the numbers indicate the location for fresh-tissue scleral thickness measurements. The optic nerve is excised approximately 2 mm behind the eye and left in place during testing. The apex tracking location is immediately on the nasal and temporal side of the optic nerve, and DIC measurements are made in locations every 100 micrometers from there toward the fixture attachment at the limbus.

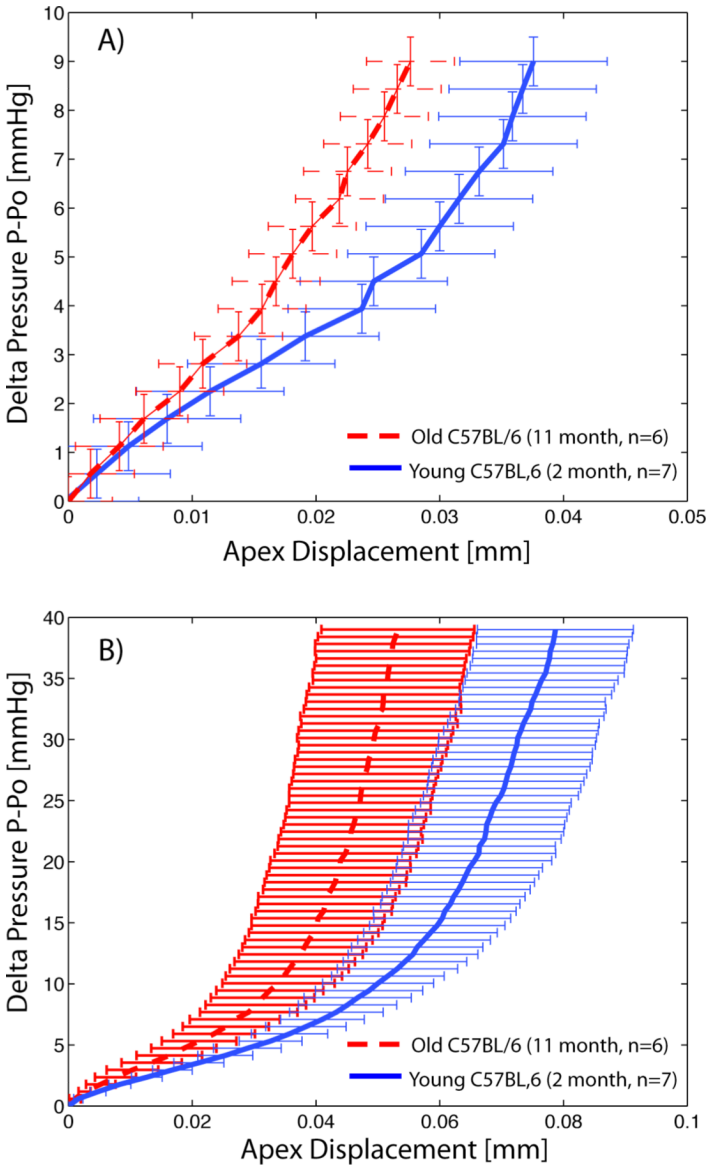

Figure 4.

The averaged apex displacement, representing an average of two points from the peripapillary region for each specimen, comparing the 2 and 11 month old C57BL/6 scleral tissue for A) the first loading ramp from 6 to 15mmHg and B) the last loading ramp from 6 to 45mmHg. Age has a significant stiffening effect to the structural response of the inflating mouse sclera.

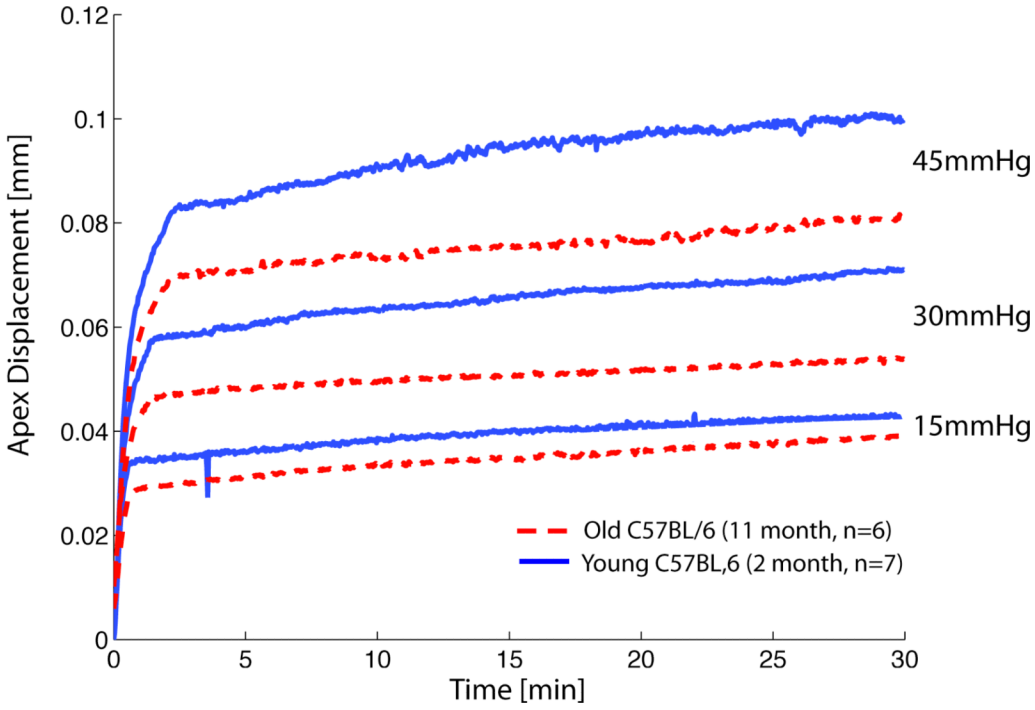

Figure 5.
The averaged creep response of the 2 and 11 month old C57BL/6 scleral tissue to elevations in pressure. The younger tissue showed evidence of pressure-dependent creep, where the older tissue did not. The associated creep rates are reported in Table 4.

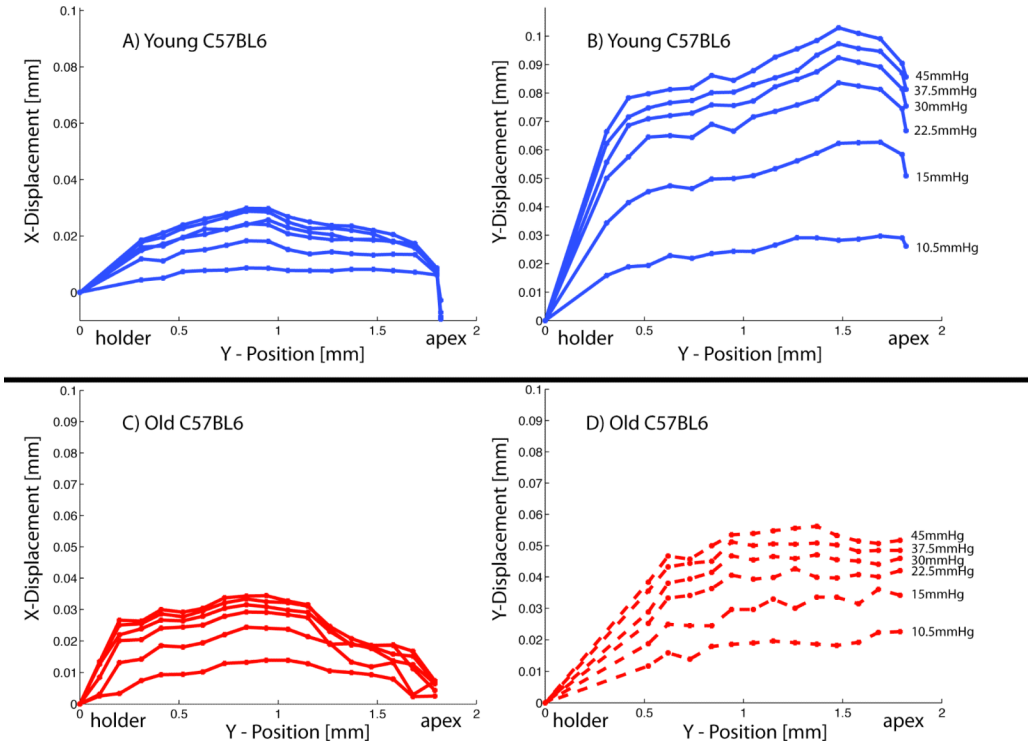

Figure 6.

Sclera inflation displacement profiles following tracking points from the limbus (testing fixture) to the apex for a typical 2 month old C57BL/6 sclera in the A) *x*-direction B) *y*-direction, and a typical 11 month old C57BL/6 sclera in the C) *x*-direction D) *y*-direction. Profiles are taken at 10.5, 15, 22.5, 30, 37.5, and 45mmHg.

Table 1

Diameters of the enucleated mouse eye

Mouse Age	Anterior –Posterior	Nasal –Temporal	Inferior –Superior
2 month (*n* = 10)	3.26 ± 0.11	3.13 ± 0.07	3.11 ± 0.09
11 month (*n* = 9)	3.49 ± 0.05	3.39 ± 0.07	3.34 ± 0.13

Measurements in millimeters, mean ± standard deviation

Table 2

Fresh scleral thickness measurements showing regional variation from the limbus to the ONH

Group	Peripapillary Region 1	Region 2	Region 3	Region 4	Region 5	Limbus Region 6
2 month inflated (*n* = 7)	64.7 ± 4.7	48.0 ± 5.5	41.1 ± 4.0	36.7 ± 4.7	34.4 ± 3.3	53.8 ± 5.4
11 month inflated (*n* = 6)	63.4 ± 7.0	49.5 ± 5.9	41.8 ± 3.6	36.1 ± 2.5	34.8 ± 4.8	57.1 ± 6.4
2 month uninflated (*n* = 7)	64.5 ± 2.9	49.1 ± 4.9	39.2 ± 2.6	36.9 ± 2.8	36.2 ± 6.8	60.3 ± 3.7
11 month uninflated (*n* = 6)	64.2 ± 3.1	46.9 ± 4.5	42.1 ± 3.5	37.2 ± 2.3	36.1 ± 3.1	56.5 ± 6.2

Measurements in micrometers, mean ± standard deviation

Table 3

Stiffness of the pressure-displacement response measurements showing a stiffening effect with pressure

Mouse Age	Po-15 mmHg	15-22.5 mmHg	22.5-30 mmHg	30-37.5 mmHg	37.5 – 45 mmHg
2 month (*n* = 7)	193 ± 40	499.7 ± 46	1106.2 ± 101	1491.1 ± 135	1453.5 ± 139
11 month (*n* = 6)	287 ± 100	741.8 ± 130	1436.8 ± 187	2293.5 ± 290	2381.0 ± 290

Data are given in mmHg/mm, and represent the structural stiffness in the different pressure regimes during the last ramp-hold test to 45mmHg. The tolerance represents the combined error of the pressure transducer and the standard deviation of displacement responses.

Table 4

Creep Rates During Ramp Hold Tests

Mouse Age	Set pressure		
	15mmHg	30mmHg	45mmHg
2 month (*n* = 7)	0.4 ± 0.2	0.5 ± 0.1	0.6 ± 0.2
11 month (*n* = 6)	0.4 ± 0.1	0.3 ± 0.3	0.4 ± 0.2

Data are given as micrometer/minute, mean ± standard deviation